Sediment delivery to sustain the Ganges-Brahmaputra delta under climate change and anthropogenic impacts

Jessica Raff, Steven Goodbred, Jennifer Pickering, Ryan Sincavage, John Ayers, Md. Saddam Hossain, Carol Wilson, Chris Paola, Michael Steckler, Dhiman Mondal, et al.

TITLE

Sediment delivery to sustain the Ganges-Brahmaputra delta under climate change and anthropogenic impacts

AUTHOR LIST

Jessica L. Raff (jessica.l.raff@vanderbilt.edu) [a*], Steven L. Goodbred, Jr. (steven.goodbred@vanderbilt.edu) [a*], Jennifer L. Pickering (jlpckrng@memphis.edu) [b], Ryan S. Sincavage (rsincavage@radford.edu) [c], John C. Ayers (john.c.ayers@vanderbilt.edu) [a], Md. Saddam Hossain (mhssain7@memphis.edu) [c], Carol A. Wilson (carolw@lsu.edu) [d], Chris Paola (cpaola@umn.edu) [e], Michael S. Steckler (steckler@ldeo.columbia.edu) [f], Dhiman R. Mondal (dmondal@mit.edu)[h], Jean-Louis Grimaud (jean-louis.grimaud@mines-paristech.fr) [l], Celine Jo Grall (celine.grall@univ-lr.fr)[f,j], Kimberly G. Rogers (kgrogers@colorado.edu) [k], Kazi Matin Ahmed (kmahmed@du.ac.bd) [l], Syed Humayun Akhter (shakhter@bou.ac.bd) [m], Brandee N. Carlson (bncarlson@uh.edu) [n], Elizabeth A. Chamberlain (liz.chamberlain@wur.nl) [o], Meagan Dejter (meagan.dejter@gmail.com) [a], Jonathan Gilligan (jonathan.gilligan@vanderbilt.edu) [a], Richard P. Hale (rphale@odu.edu) [p], Mahfuzur R. Khan (m.khan@du.ac.bd)[l], Md. Golam Muktadir (golam.muktadir@bup.edu.bd) [q], Md. Munsur Rahman (mmrahman@iwfm.buet.ac.bd) [r], Lauren A. Williams (lauren.williams@energy.virginia.gov) [a]

AFFILIATIONS

[a] *Department of Earth and Environmental Sciences, Vanderbilt University, Nashville, TN, USA*

[b] *Center for Applied Earth Science and Engineering Research, The University of Memphis, Memphis, TN, USA*

[c] *Department of Geology, Radford University, Radford, VA, USA*

[d] *Department of Geology and Geophysics, Louisiana State University, Baton Rouge, LA, USA*

[e] *Department of Earth and Environmental Sciences, St Anthony Falls Laboratory, University of Minnesota, Minneapolis, MN, USA*

[f] *Lamont-Doherty Earth Observatory, Columbia University, Palisades, NY, USA*

[h] *Haystack Observatory, Massachusetts Institute of Technology, Westford, MA, USA*

[i] *Centre de Géosciences, PSL University/ MINES Paris, Fontainebleau, France*
[j] *CNRS - Littoral Environnement et Sociétés, La Rochelle University, La Rochelle, France*
[k] *Institute for Arctic and Alpine Research, University of Colorado, Boulder, CO, USA*
[l] *Department of Geology, University of Dhaka, Dhaka, Bangladesh*
[m] *Bangladesh Open University, Board Bazar, Gazipur, Bangladesh*
[n] *Department of Earth and Atmospheric Sciences, University of Houston, Houston, TX, USA*
[o] *Soil Geography and Landscape, Wageningen University, Wageningen, Netherlands*
[p] *Department of Ocean & Earth Sciences, Old Dominion University, Norfolk, VA, USA*
[q] *Department of Environmental Science, Bangladesh University of Professionals, Dhaka, Bangladesh*
[r] *Institute of Water and Flood Management, University of Engineering and Technology, Dhaka, Bangladesh*

ABSTRACT

The principal nature-based solution for offsetting relative sea-level rise in the Ganges-Brahmaputra (G-B) delta is the unabated delivery, dispersal, and deposition of the rivers' ~1 billion tons of sediment. Recent hydrological transport modeling suggests that strengthening monsoon precipitation in the 21st century could increase this sediment delivery 34-60%; yet other studies demonstrate that sediment could decline 15-80% if planned dams and river diversions are fully implemented. We validate these modeled ranges by developing a comprehensive field-based sediment budget that quantifies the supply of Ganges and Brahmaputra river sediment under varying Holocene climate conditions. Our data reveal natural responses in sediment supply comparable to previously modeled results and suggest that increased sediment delivery may be capable of offsetting accelerated sea-level rise. This prospect for a naturally sustained G-B delta presents possibilities beyond the dystopian future often posed for this system, but the implementation of currently proposed dams and diversions would preclude such opportunities.

INTRODUCTION

Only in the past few years have global assessments of river-delta response to accelerated sea-level rise and declining sediment supply utilized datasets more complete [5,6] than the single mean values often used in earlier studies [7–9]. Most earlier assessments yield grave predictions for the response of deltas to climate change and human-related impacts, and while those concerns are not unfounded, they generally oversimplify complex system behaviors and can thus mask potentially more positive delta scenarios [6]. One risk of such negative but simplified assessments is to foster dystopian narratives that uphold engineering structures as the key defense against climate change, thereby undermining local to regional efforts to maintain sediment supply and preserve land in these low-lying landscapes [7,10].

A robust supply of clastic sediment is the principal nature-based resource for offsetting relative sea-level rise in river deltas, yet better constraints and data availability on the delivery and dispersal of sediment are needed[11] to ensure that future delta scenarios accurately account for both dynamic natural-system behavior [12] and the continuing impacts of development and land-use change. Furthermore, it is increasingly important that coupled human-natural approaches be used to predict delta fate, because as many as 630 million people currently live in regions that may be uninhabitable by 2100 due to relative sea-level rise (RSLR), flooding, and inundation [13]. Recent global delta studies using highly resolved, spatially and temporally varying data inputs indeed suggest that more deltas than generally recognized have been gaining land and that deltas overall may be collectively more robust than previously thought [6,14–16].

These recognitions are important because the fate of river deltas and their growing populations are closely tied to riverine sediment supply [14], which has a direct effect on land reclamation efforts, household migration decisions, and the ability to occupy marginal (vulnerable) lands [17–19]. For instance the relocation of >20,000 Rohingya refugees to a newly emergent tidal island in the Ganges-Brahmaputra river-mouth estuary is a vivid example involving each of these issues[20,21]. In fact, the Bangladesh Delta Plan 2100 proposes numerous coastal barriers (i.e., cross-dams) to trap sediment in the same region and accelerate the growth of new land for potential reclamation and human occupation. The social, engineering, and political challenges of relocating displaced communities to emergent lands

notwithstanding, a pre-requisite for coastal land reclamation remains the uninhibited delivery of Ganges-Brahmaputra (G-B) river sediment and its effective dispersal across the coastal zone.

Among the world's river deltas, the G-B system presents an important example of deltaic response to climate change and sea-level rise due to its naturally large sediment supply, (currently) limited upstream damming, and an immense basin population of ~500 million people [35]. The basin's hydrology, climate, and sediment transport are controlled by the seasonal South Asian monsoon, the strength of which varies considerably over decadal to millennial timescales [36–38]. Indeed, both modeling and proxy records document large fluctuations throughout the Holocene, with high precipitation in the early Holocene followed by a general reduction after ~8 ka and a smaller increase in the last millennium or two [39–45]. For the coming century, the most recent IPCC AR5 and AR6 reports continue to predict increased and more variable monsoon precipitation by 2100 under nearly all representative GHG concentration pathways (RCPs) [46,47]. Such increases may be comparable to periods of stronger monsoon earlier in the Holocene, and thus provide a possible analog for future responses. In addition to the strengthening of monsoon precipitation, regional warming may also enhance the melting of Himalayan glaciers and further increase discharge and sediment loads for at least the coming decades or century [3,48.]

Observation-based estimates for the supply of sediment currently delivered to the G-B delta range from <500 to >1,100 Mt/yr (Mt = 10^6 metric tonnes), representing considerable uncertainty and a critical knowledge gap for projecting delta response to sea-level rise [11,28–30]. Looking forward, recent modeling studies by Darby et al. (2015) [1], Dunn et al. (2018) [2] and Higgins et al. (2018) [3] each consider future changes in G-B sediment supply and their potential consequences for the delta. Their findings suggest historically unprecedented levels of change in sediment supply from the Ganges and Brahmaputra rivers are possible over the next 50–100 years, either through reductions from damming and diversions (e.g., Higgins et al. 2018)[3], increases from strengthened monsoon precipitation and river discharge (e.g., Darby et. al., 2015; Fischer et al., 2017)[1 11], or a combination of these factors (Dunn et al. 2018; Tessler et al., 2018)[2]. The modeled changes, although large (±50-90%), are comparable to other Asian river systems that have undergone large changes in sediment load over the past century [4,26,27].

Toward a validation of such model projections of future sediment delivery to the G-B, we present a highly resolved, mass-balanced sediment budget that: (a) utilizes over 6,000 new field-based measurements from 500 locations (Figure 1) to provide (b) ground-truthing for modeling studies and (c) a holistic view of river system connectivity from the Himalayan source terrains to deltaic continental margin [22,23]. The budget is primarily derived from unpublished borehole data, sediment volume, mass, grain size, and provenance, all supplemented by a compilation of data from over 15 other studies (Tables 1, 2, S1). In addition to greatly improved spatiotemporal resolution, this new work is distinct from previous G-B mass budgets [24,25] that lacked any information on the river source (i.e., provenance) or grain-size distribution of stored sediments. Both data types introduced here yield valuable results on total bedload contribution to the delta and the varying and asymmetric delivery of sediment from the two main rivers in response to climate change. To our knowledge, no mass balance of comparable detail and longevity exists for a major river delta, thus providing an unparalleled perspective on natural-system response to climate change and an opportunity to ground-truth modeled responses under future climate scenarios.

Here we carefully quantify past changes and compare them with the sediment demands that will be required for the G-B delta to offset projected increases in sea-level rise in the coming century. Our work explores the validity of these sediment-delivery projections through comparison with sediment-load responses to Holocene climate change and monsoon strength. From field data we reconstruct the mass and grain-size distribution (caliber) of sediment sequestered in the delta through the Holocene and how that mass was distributed and stored to build the delta system.

RESULTS AND DISCUSSION

Total Delta Sediment Composition

Reconstructed sediment storage rates from the stratigraphic record represent minimum total riverine sediment loads (bedload and suspended load) delivered to the G-B delta. Unless otherwise noted, sediment delivery will be used to refer to sediment loads reconstructed from stored Holocene sediments. The total mass of sediment stored in the G-B basin over the

Holocene (12—0 ka) is >1.2 × 10^7 Mt (Table 1), which averages to a minimum mean delivery rate of ~1000 Mt/yr and is comparable to the oft-cited modern load of ~1100 Mt/yr. The grain size of sediment stored in the delta is approximately equally apportioned across muds (<62.5 µm – 30%), very fine to fine sand (62.5–250 µm – 39%), and medium to coarse sand (250–1000 µm – 31%) (Table 1). For this study, we conservatively classify sediments <250 µm (muds to fine sand) as suspended load and larger particles 250–1000 µm as bedload [31,49]. These delineations result in Holocene delta deposits comprising ~70% suspended load and 30% bedload sediments, considerably exceeding not only the 10% bedload transport rate often presented in the literature but even high estimates typically placed at 20% [31–33,50]. The significance is that much of the long-term construction of the delta has been through the aggradation of bedload sand, which is highly susceptible to upstream trapping in reservoirs and thus an important consideration for future management of the delta [4]. Moreover, the bedload plays a disproportionate role in the growth of bars and other locally elevated river topography upon which many village communities are sited.

Variable Holocene Sediment Storage

Despite similarity between the average modern and Holocene rates for sediment reaching the delta, sediment delivery over millennial timescales varies by >200% from lowest delivery rates of 850 Mt/yr through the mid-late Holocene (6–0 ka) up to maximum delivery rates in the early Holocene of 1200 Mt/yr (8–6 ka) to 2000 Mt/yr (10–8 ka) (Table 1; Figure 2). Fluvial sediment began aggrading in the delta beginning ~12 ka at a rate of ~820 Mt/yr (12–10 ka) but delivery increased to at least 2000 Mt/yr (double the modern load) during the period of strongest monsoon from 10–8 ka. These results confirm previous findings that the Ganges and Brahmaputra rivers carried a sediment load at least twice as large as the modern for over two millennia. This large supply supported aggradation on the delta sufficient to offset very high rates of sea-level rise that averaged >1 cm/yr over this period. These high early Holocene rates of sediment delivery and sea-level rise are comparable to those anticipated for the next century based on the Darby et al. [1] modeling for sediment supply and IPCC projections for sea-level rise [51]. These similarities between our paleo-reconstructions and the modeled futures of other

studies highlight a potential scenario of sediment supply whereby the delta may be able to maintain itself against increases in sea-level rise over the next century.

Emphasizing that our budget reconstructions represent minimum supply rates, the portions of the sediment load lost through transport to the Swatch of No Ground canyon and G-B fan are not included in the Holocene sediment delivery rates. Such sediment bypass would have been greatest from 12–8 ka when the river channels were constrained to their lowstand valleys and discharged directly to the canyon head. Simple reconstructions of mud deposition in the Swatch of No Ground and active channel of the G-B Fan [52–54] suggest that as much as another ~200 Mt/yr of sediment may have been delivered by the rivers in the early Holocene. After 8 ka, though, most sediment delivered to the margin was efficiently trapped in the delta and accounted for in our sediment budget, as reflected in part by the abrupt drop in sedimentation on the G-B Fan after 9 ka despite continued high river discharge [52–54]. Interestingly, it is during this period of effective sediment trapping that the sediment budget reveals an average long-term sediment load of ~850 Mt/yr, which is slightly above half of the modern supply and indicates that the G-B rivers responded as acutely to monsoon weakening as they did for strengthening in the early Holocene.

In addition to variation in total mass delivered, the sediment loads between 12–10 ka and 10–8 ka are considerably coarser than the Holocene average and comprise ~40% medium to coarse sand presumably transported as bedload (Table 1). In contrast, the proportion of bedload transported to the delta decreases to ~20-25% after 8 ka. In all, this fraction of bedload comprising delta stratigraphy is more than double the estimated modern value of 10% or less of the measured total load [31–33,50]. However, we do not anticipate that future sediment supply would be as coarse as these deposits, even under a strengthened monsoon. Nevertheless, the importance of sand delivery by these large braided rivers for future delta stability should not be undervalued, particularly in context of the massive mining of river sands occurring in the G-B and other rivers worldwide [55,56].

Ganges and Brahmaputra Sediment Provenance

Using bulk Sr concentration of stored sediments, which has been shown to be a reliable indicator of river source in this system [57–59] (Figure S3), we have quantified the fraction of sediments delivered to the delta by the Ganges, Brahmaputra, and smaller local rivers. Results for the Holocene show that nearly 54% of sediments were sourced by the Brahmaputra, ~30% by the Ganges, and the remaining ~14% by local rivers including the Tista river in northwest Bangladesh and others draining the Indo-Burman fold belt and Shillong Massif to the east (see Methods for further details). Both major rivers demonstrate considerable variability in sediment delivery throughout the Holocene, but responses are more pronounced for the Brahmaputra catchment (Table 2, Figure 2). Since 10 ka, the long-term averages for Ganges sediment load ranges 308 to 426 Mt/yr, which is comparable to the variance in modern load estimates of 300–450 Mt/yr [30,60,61]. This suggests that Ganges discharge has been relatively stable even with considerable regional climate variability, a finding that is consistent with the similarly modest response projected by Darby et al. (2015) under future climate scenarios. Note that the low Ganges value of 116 Mt/yr stored from 12–10 ka (Table 2) is likely an underestimate due to sediment bypassing, as sedimentation on the G-B fan remained high at this time [52,54].

In contrast, sediment load for the Brahmaputra has been highly variable over the Holocene, with a 4-fold range from a high of ~1100 Mt/yr at 10–8 ka to a low of ~370 Mt/yr from 6–0 ka. Relative to the Brahmaputra's modern load of 500–650 Mt/yr, these values represent a long-term doubling and halving over the Holocene, respectively, reflecting acute response to monsoon strength and related sediment production and transport processes. As for the Ganges, the magnitude of response for our Brahmaputra reconstructions is similar to the projections made by Darby et al. (2015), lending confidence to their results of increased, but differential, future sediment transport for each river. In particular, the differing response of Ganges and Brahmaputra sediment load to climate change will remain highly relevant to managing the G-B delta, given that the largest sediment-source areas for the two rivers lie in India and China, respectively.

Response to monsoon variability

The modeling of river discharge under future climate change suggests that increases in G-B sediment load of 34-60% [1] are possible, which would be a substantial increase in sediment delivered to the G-B delta and thus a potentially important buffer against accelerated rates of sea-level rise. These modeled values are supported by our findings from the early Holocene period (12–8 ka) of strengthened monsoon, when fluvial sediment loads were enhanced for both river systems compared to periods of weaker monsoon from 8–0 ka. Between periods of stronger and weaker monsoon conditions, Brahmaputra discharge varied from 370-1100 Gt/yr377-1119 Mt/yr (i.e., a ±2-fold difference from modern), whereas the Ganges varied only 308-426 Mt/yr (i.e., a range comparable to modern estimates). Note we do not include here the low Ganges value of 116 Mt/yr for the 12-10 ka period due to presumed sediment bypassing at this low sea-level stage.

Our sediment budget reconstructions are also consistent with the results of Darby et al.[1] further suggesting that the Brahmaputra river catchment is considerably more sensitive to changes in climate, and that during wetter periods it is the more dominant source of sediment to the delta. Importantly, there is no overlap in methods between our paleo-reconstructions and the forward-looking projections of Darby et al. (2015) [1], suggesting that the comparable results provide a reasonable reflection of G-B system dynamics. Among the reasons for such an acute response from the Brahmaputra relative to the Ganges is the catchment's proportionally smaller lowland area [1] that limits its capacity for sediment storage. This reduced buffering capacity means that variations in sediment yield from the Brahmaputra catchment reach the delta more quickly and with less attenuation than those from the Ganges catchment [22]. Another factor contributing to acute response of the Brahmaputra sediment supply to climate is the catchment's large area of relatively arid and sparsely vegetated highlands in Tibet, where modest changes in the water budget can drive much higher or lower erosion rates [62]. Moreover, recent (2003–2008) loss of glacial elevation in the Himalayan catchments [63] introduces glacial melt as another source of increased discharge and sediment delivery, although persistence of this contribution may wane beyond 2100 as ice extent contracts [3].

In contrast to the Brahmaputra, the Ganges catchment lies at the center of the South Asian monsoon system with robust precipitation and vegetation across the Himalayan front range, which is where most sediment and water discharge are generated. The Ganges also hosts a vast foreland filled by alluvial mega-fans that are capable of storing sediment; however, their ability to buffer short-term changes in sediment supply is limited because many fan channels in the Ganges basin are incised and decoupled from the adjacent plains, or are otherwise heavily embanked like the Kosi River fan, causing greater downstream bypass of sediment [50,64]. Indeed, during the early Holocene when the monsoon was strong, the Ganges system incised and remobilized megafan sediments that had aggraded in the early post-glacial period[64–66]. These phenomena in the Ganges catchment support results from models indicating that variable water supply (e.g. due to fluctuations in monsoon strength) can cause periods of aggradation when water flux decreases and periods of incision when water flux increases[67]. Overall, the Ganges fan systems serve to buffer variance in sediment supply as compared with the Brahmaputra that has proportionally less lowland storage area, which is well reflected in both our Holocene reconstructions and the Darby et al.[1] scenarios for the next century.

Given interest in the potential increase in sediment load under future climate scenarios, it is important to also consider the timescales at which sediment stored in the upper catchment may be remobilized from hillslope, valley, and floodplain settings and delivered to the delta. Our paleo-reconstructions do not provide great precision on those timescales, but evidence from both the G-B and the Indus delta systems show that changes in the supply of riverine sediment load respond to monsoon precipitation at timescales less than the sub-millennial resolution of radiocarbon-dated stratigraphic sections [25,68]. Such short response times would indeed be consistent with hydrologically driven changes in transport and an abundance of available sediment (i.e., a transport limited system) [67]. Indeed ~95% of the G-B sediment load is delivered during the summer monsoon and resulting period of high river discharge (May–October). In this context, more precipitation over the catchment readily remobilizes abundant sediment stored as hillslope regolith and alluvial deposits in the upper catchment. Modern examples also appear to confirm rapid sediment transfer from upland source areas to the Bengal margin, perhaps best exemplified by the decadal-scale transport and delivery of

290 Brahmaputra bedload introduced by 100s of landslides generated in the major 1950 Assam
291 earthquake (M 8.6) [69,70]. Similarly, HydroTrend, the climate-driven hydrological water balance
292 and transport model used by Darby et al. (2015) to consider future basin response to increased
293 precipitation, does not suggest any significant lag time for the delivery of G-B sediment to the
294 delta [1].
295
296 **Can increased supply support sediment needs?**
297 To better understand the implications of varying sediment load and rates of sea-level rise
298 on delta sustainability, we have produced mass balance estimates under a variety of past,
299 present, and future scenarios (Figures 3 and 4). The $\Delta Mass$ rates (Mt/yr) represent the annual
300 excess (>0) or deficit (<0) supply of sediment for each scenario, and the $f_{(supply)}$ is the fractional
301 excess or deficit of delivered sediment specifically for the medium-demand scenario. Results
302 show an excess of sediment delivery under most natural conditions during the Holocene and
303 modern, even during periods of rapid sea-level rise comparable to the rates anticipated for the
304 coming century (5 to 12.5 mm/yr). The modern mass delivery also readily meets demand using
305 the most often reported sediment load value of 1100 Mt/yr, but the delta would be facing a
306 measurable deficit if the occasionally cited value of 700 Mt/yr were correct [28–30,60]. Given the
307 G-B delta's persistent growth in land area over the last few decades and centuries [71–73], the
308 higher value of 1100 Mt/yr appears to be more accurate. For the future, unabated sediment
309 delivery in the 2050 and 2100 climate-only scenarios yield a $f_{(supply)}$ ranging from a slight to
310 moderate deficits of 7-20%, meaning that erosion rates and land loss may be correspondingly
311 slow and provide valuable time for mitigation strategies to be implemented. These mass
312 balance results (Figure 3) are consistent with persistent growth of the delta from Holocene to
313 modern and are not simply optimistic calculations. Rather, these reconstructions and future
314 scenarios emphasize natural resilience of the G-B delta linked to the region's robust monsoon
315 precipitation and high sediment yield from the tectonically active Himalayan Mountains.
316 Evidence of a robust and resilient G-B delta has received less attention than scenarios
317 considering a heavily engineered future, where major sediment reductions and high rates of
318 land loss are likely – yet both outcomes are plausible, and the eventual pathway is more

contingent on the decisions of policy makers than on climate change. Indeed, our mass balance estimates (Figure 3) show massive sediment deficits of more than 100% to over 2000% under all future scenarios that consider widespread dam construction and water diversions. These futures are the ones that will more aptly compare the G-B delta with the catastrophic land loss already occurring in the Mississippi, Nile, Indus, Mekong, and other deltas fed by heavily dammed rivers [9,74,75]. Thus, the G-B delta is not doomed to drown under climate change – it is doomed to drown under scenarios of anthropogenic reductions in the delivery and dispersal of sediment to the delta[76].

Many damming and diversion plans for the G-B rivers have been developed but not yet widely implemented [3], thus presenting a window of opportunity to better steward the G-B delta future. A major risk of not acknowledging the G-B delta's intrinsically robust sediment supply and potential resilience against rising sea level is that environmental managers will otherwise plan for the dystopian future of a drowning landscape and the development of policies that steer toward this anticipated outcome of ruin [10,77].

Although the potential for considerably enhanced sediment delivery to the G-B delta exists, it alone would still be insufficient to sustain the system. Rather, delivered sediment must also be allowed to freely disperse to regions of the delta where it is needed to offset subsidence and rising sea level. Within the G-B delta itself, widespread embankments in the tidally influenced coastal zone already limit such sediment delivery to poldered islands [78] and have exacerbated local sea-level rise [79]. Potentially sustainable efforts to manage sediment accretion in these embanked polders are underway but still face implementation challenges [14,80,81].

In contrast, in natural areas of the delta such as the Sundarbans mangrove forest, a protected UNESCO World Heritage site, and the Meghna (G-B) River mouth estuary, unhindered sedimentation is rapid and is readily keeping pace with effective sea-level rise (0.5-1.5 cm/yr) [76,82,83]. In fact, in the rivermouth estuary, low barriers (i.e., cross dams) built across shallow waterways have been effective at trapping sediment and rapidly converting open water to emergent intertidal and supratidal lands. Such land reclamation projects are a key part of Bangladesh's plans for mitigating the effects of sea-level rise, but the success will require the continued uninhibited delivery and dispersal of sediment. Even under scenarios of enhanced

sediment delivery, maintaining these natural morphodynamic processes will remain an essential ingredient for long-term sustainability of the delta, which cannot be fully managed or hardened given its size, complexity, and large mass and energy inputs [12,84].

Anthropogenic threats to future sediment delivery

Despite projected increases under a strengthened monsoon, anthropogenic factors may yet dominate the system-scale responses and drive sediment loads to be considerably lower. Specifically, plans across South Asia for hydropower development and interbasinal watershed management portend major reservoir construction and water diversions in the coming century [3,85]. Modeling of the impact of these activities on the river basins suggests moderate (30%) to extreme (88%) decreases in sediment discharge under a range of plausible river-management scenarios [2,3] (Figure 3). Existing studies focus on the impact of India's National River Linking Project (NRLP) and hydropower projects in Nepal, both of which disproportionately affect the Ganges river system [2,3]. No study has yet assessed the potential impact of China damming the Yarlung Tsangpo [85], which is the primary water and sediment source for the Brahmaputra.

Uncertainty in the G-B delta sediment budget hinders the ability to create sustainable development plans [11] and makes it possible for upstream decision-makers to justify continued dam construction and water diversions [86–89] at the expense of downstream sediment supply to the delta [86,90]. Reduced sediment supply will threaten delta stability, particularly if loads decrease below those needed to maintain the delta surface above sea level [80,82]. In other mega-deltas like the Mekong and Mississippi, reduced sediment loads from damming and sand extraction have already led to increased saltwater intrusion, decreased soil fertility, loss of land area with rising sea level, and elevation deficits that increase susceptibility to flooding and storm surges [9,74,75].

Amidst typically negative risk assessments of the G-B delta, it is rarely acknowledged that the system has persistently gained several km^2/yr of land-surface area for at least the last several centuries, a pattern that continues today without any sign of waning [76,84]. With the next century of climate change, models indicate that the delivery of sediment to the delta will not only persist but likely increase considerably, with the potential to offset accelerating rates of

sea-level rise [1,11]. Such projections are consistent with the Holocene sediment reconstructions presented here (Figures 2 and 3), and these results collectively suggest that the G-B delta may be among the world's most naturally resilient large coastal systems.

The magnitudes of sediment delivery suggested by our field-based reconstructions and the modeled natural scenarios are very similar, suggesting that the results are reasonably robust; however, even if future increases in sediment load are less than suggested here, a key point is that any increase in sediment supply will help mitigate the impacts of sea-level rise and delay delta drowning. With global warming and sea-level rise baked into the climate system for centuries, any factors such as increased sediment delivery that can delay or reduce impacts may be critically important for effective and manageable human responses.

Importance of perception to delta futures

Increased sediment delivery under a strengthened monsoon supports the possibility for a more favorable G-B delta outcome under a majority of future climate scenarios. These natural-system responses to climate variability support conclusions from future model scenarios for the coming century [1,91] and modern field-based studies [76,82] that the G-B delta is not inherently doomed to drown. Instead, proper management of sediment resources, particularly within at-risk coastal regions [78,80], may provide security for coastal populations and livelihoods often presented as unviable under future climate scenarios[10,77,92,93]. However, the persistence of a doomed-to-drown narrative for Bangladesh may perpetuate dystopian views in which particular regions of the delta or livelihoods are considered unsustainable and thus become subject to maladaptive policies [77]. Such perceived threats shift the focus of mitigation projects toward the strengthening or expanding of hard infrastructure, approaches that have already disrupted sedimentation processes and undermine the delta's natural resilience to sea-level rise [12]. The resulting impacts may exacerbate the displacement of households and increase migration away from these supposedly unsustainable coastal locations [10]. Although hard-engineering responses may continue to be part of a sensible coastal management plan, adopting them under threat of a dystopian future may steer policies away from more nature-based solutions and other

sustainable development policies that would bolster long-term stability of the coastal zone through the effective management of sediment delivery and dispersal.

Upstream of the delta, though, a key concern is how the supply of sediment reaching the delta will be impacted by anthropogenic activities in the catchment basin. In other words, any natural increase in sediment delivery resulting from increased monsoon precipitation [1,91] will compete with anthropogenic decreases caused by the construction of proposed dams and water diversions upstream of the delta[2,3,80]. In all, the work presented here and by others [6,76] offers the possibility for a more optimistic future that is often absent in the literature and media coverage of the G-B delta. The emerging narrative on fate of the delta shifts somewhat away from climate change and more toward the sustainable management of water and sediment resources, both in the upstream catchment and across the delta itself. The caveat is that the G-B delta may be more resilient to climate change only in the absence of major dam construction and water diversions upstream of the delta and major disruptions to the effective delivery and dispersal of sediment across the delta and coastal zone.

METHODS

Data source

The sediment budget is produced from a largely unpublished dataset of sediment grain-size and geochemistry measured on 6,100 sediment samples from 455 boreholes collected by the authors and colleagues between 2011-2021. The boreholes have a maximum depth of 95 m and were collected in 23 transects across the delta. The stratigraphy for about half of these cores (~200) has been published in five previous papers [94–98], the radiocarbon ages are published in Grall et al. (2020), and local grain-size and mass-balance for one sub-basin of the delta published in Sincavage et al. (2019). These data are supplemented by widespread core and seismic data previously published by Ahmed et al. (2010), Bangladesh Agriculture Development Corporation (1992), Shamsudduha et al. (2008), Pate et al. (2009), Department of Public Health Engineering and Japanese International Cooperation Agency (JICA) (2006), JICA (1976), Ghosal et al. (2015), Hait et al. (1996), Hoque et al. (2012), Hoque et al. (2014), Khan & Islam (2008), Michels et al. (1998), Palamenghi et al. (2011), and Sarkar et al. (2009) [99–113]. These

supplemental data extend across the entire Bengal Basin, including the continental shelf and West Bengal, India where we do not have samples. The complete compilation of data from these sources adds 3,720 sites to the more detailed results from our 455 cores.

Field and laboratory methods

Sediment samples for the cores in this study were collected at 1.5-m depth intervals and photographed, described, and packaged in the field [95–97]. In the lab, every third sample with depth as well as samples at sedimentologic contacts were analyzed for grain-size distribution using a Malvern Mastersizer 2000E particle size analyzer at ¼ φ intervals from clays (0.49 μm) to coarse sands (1000 μm). Samples were also analyzed for bulk geochemistry by X-ray fluorescence using a portable Thermoscientific Niton XL3 Analyzer (pXRF), which returns information on composition of both major and trace elements in the sediments. Strontium concentrations from the XRF results are used to document sediment provenance following published methods [114], effectively distinguishing sediment deposited by the Ganges, Brahmaputra, mixed Ganges-Brahmaputra, or other local river sources [57–59] (Figure S3). Sediments having higher bulk Sr values >130 ppm are derived from the Brahmaputra basin, which drains mafic batholiths along the Tsangpo suture zone, compared with lower bulk Sr values < 110 ppm for the Ganges (in central and western G-B) or local sediment sources in the north (Tista River), northeast (Shillong Massif), and east (Indo-Burman Fold Belt). Of the 6100 samples analyzed to date for grain size and geochemistry, over 4,000 are Holocene-aged and included in this study.

Mapping

Mapping of Holocene G-B delta deposits was performed using ArcGIS. The Holocene-Pleistocene boundary depth was identified using sediment grain size, color as a proxy for oxidation state, and radiocarbon data from the aggregated dataset [94–96,105,115–117] and supplemented with depth data from cores, wells, and seismic data in reports and previously published studies [99–112]. Simple co-kriging was used to create an interpolated prediction surface of the depth to the Pleistocene boundary from both the hand drawn contours and depth

information from >950 core sites and hundreds of kilometers of seismic lines from many studies [99–112]. To synthesize the data from these 6000+ samples and to control for variance related to regional tectonics and structure, antecedent Pleistocene topography, and the backwater and coastal transition, we partitioned the delta into 9 physiographic and depositional regions based on similarities in processes and inputs (see Fig. S2). Several of these regions are parsed further into sub-regions, largely based on the core-data distribution, to increase the sediment budget resolution and to account for downstream fining and fluvial depositional processes. The main provinces include the Jamuna valley, Ganges valley, Sylhet basin, Meghna valley, Fold Belt, Madhupur Terrace, West Bengal, Interfluve, and Offshore. We then regroup these sub-regions into valleys (Jamuna valley, Ganges valley, Meghna valley), interfluves (Madhupur Terrace, Paleo-interfluve, Fold Belt, West Bengal), and basins (Offshore, Sylhet Basin). To better understand the subsurface stratigraphy, we calculated the grain-size distribution of all samples by 5-m depth bins within spatiotemporal units and then multiplied by the total sediment mass in that unit to yield the sediment-mass grain-size distribution by depth for each region (n=251; see supplemental materials).

Due to spatially varying subsidence rates and temporally changing eustatic sea-level rise that control accommodation in the delta, simple depth conversions do not correlate well with age of the deposits. In other words, establishing well-defined time horizons from radiocarbon ages is complicated by instantaneous variations in delta surface topography. However, averaged over longer periods typical of channel avulsion and migration (i.e. 1000-2000 years), [96,118,119] a stable or growing delta system must infill accommodation generated. Therefore, the potential mass of stored sediment at any given interval will be a function of the volume created by subsidence and sea-level rise. Thus, the Holocene unit has been partitioned into Time-EQuivalent depositional units (TEQ) based on regional subsidence patterns derived from a large radiocarbon database (n>200) in Grall et al. (2018) [115] and combined with eustatic sea-level reconstructions from Lambeck et al. (2014) [120]. These relative sea-level rise controls were used to map the base-level and delta surface at 6 ka, 8 ka, 10 ka, and 12 ka. The resulting surfaces were spliced in GIS to form TEQ units that correspond to accommodation generated during the periods 6—0 ka, 6—8 ka, 8—10 ka, 10—12 ka. To calculate the delta surface over which

sediments were deposited and the volume of material stored during each TEQ, we subtracted the interpolated Holocene surface from the effective subsidence (land subsidence and sea-level rise) over those years in ArcGIS (Fig. S1, Table S1). The volume of each TEQ was multiplied by a mean bulk density based on field measurements to derive the mass of sediment stored on the delta during each TEQ. The bulk densities used range from 1.3 g/cm^3 in the shallow units to 1.8 g/cm^3 in the deepest units, and a lower value of 1.1 g/cm^3 for muddy coastal and shelf units. To calculate the grain-size distribution of each sediment package, we isolated the samples from each core contained within the TEQ, calculated the average grain-size distribution, and interpolated the grain-size distribution to the total mass of the material in each TEQ.

Offshore and West Bengal delta regions

For the offshore and West Bengal physiographic regions where we have not collected cores, we base the budget calculations on published studies. For the offshore, growth of the subaqueous delta began after ~8 ka and the stored sediment mass determined from seismic and core data [52,121]. Our budget calculations proportionally distribute 75% of this offshore delta sediment to the 6–0 ka interval and 25% to the 8–6 ka interval. The source of offshore sediment was partitioned between Brahmaputra (~60%) and Ganges (~40%) based on Sr measurements of shelf sediment by Garzanti et al. (2019) [122] and Lupker et al. (2013) [123]. The grain-size distribution of sediments stored in West Bengal is taken from previously published data in Stanley & Hait (2000) [124], who measured the mud:sand ratio to be ~70:30 in a series of Holocene-scale cores (<50 m). The average Holocene thickness of sediments in their cores was 25 m with a maximum thickness of ~45 m. Although kriging analyses show the maximum predicted thickness of Holocene sediments in West Bengal to be ~70 m, >90% of the total sediment package is stored in the upper 45 m, so the data from Stanley & Hait (2000) can be used. For comparison, our data from the G-B interfluve east of the Ganges valley and just opposite the West Bengal region is a comparable ~63% mud and ~37% sand. Since this grain-size distribution aligns well with measurements from West Bengal [124], we apply the same distribution for sediment stored in that region.

Sediment surplus and deficit calculations

A simple mass-balance model compares the mass aggradation needed to offset relative sea-level rise (RSLR) for the G-B delta with reconstructed sediment delivery rates (Figure 3). The upper delta extends from the delta apex to the slope break at the fluvial- to tide-influenced transition (Fig. S2), the lower delta from the tidal transition at the slope break to the coast, and the marine delta from the coast to base of the subaqueous delta foresets. We apply mean subsidence rates and mean eustatic sea level to each of these regions using a bulk density of 1.5 t/m^3 typical of the upper 20 m of sediment. Additional details on calculation steps are provided in Figure 3.

REFERENCES

1. Darby, S. E., Dunn, F. E., Nicholls, R. J., Rahman, M. & Riddy, L. A first look at the influence of anthropogenic climate change on the future delivery of fluvial sediment to the Ganges–Brahmaputra–Meghna delta. *Environ. Sci. Process. Impacts* **17**, 1587–1600 (2015).
2. Dunn, F. E. *et al.* Projections of historical and 21st century fluvial sediment delivery to the Ganges-Brahmaputra-Meghna, Mahanadi, and Volta deltas. *Sci. Total Environ.* **642**, 105–116 (2018).
3. Higgins, S. A., Overeem, I., Rogers, K. G. & Kalina, E. A. River linking in India: Downstream impacts on water discharge and suspended sediment transport to deltas. *Elementa* **6**, (2018).
4. Syvitski, J. *et al.* Earth's sediment cycle during the Anthropocene. *Nat. Rev. Earth Environ.* **3**, 179–196 (2022).
5. Caldwell, R. L. *et al.* A global delta dataset and the environmental variables that predict delta formation on marine coastlines. *Earth Surf. Dyn.* **7**, 773–787 (2019).
6. Nienhuis, J. H. *et al.* Global-scale human impact on delta morphology has led to net land area gain. *Nature* **577**, 514–518 (2020).
7. Tessler, Z. D. *et al.* Profiling risk and sustainability in coastal deltas of the world. *Science (80-.).* **349**, 638–643 (2015).
8. Renaud, F. G. *et al.* Tipping from the Holocene to the Anthropocene: How threatened are major world deltas? *Curr. Opin. Environ. Sustain.* **5**, 644–654 (2013).
9. Syvitski, J. P. M. *et al.* Sinking deltas due to human activities. *Nat. Geosci.* **2**, 681–686 (2009).
10. Paprocki, K. On viability: Climate change and the science of possible futures. *Glob. Environ. Chang.* **73**, 102487 (2022).
11. Fischer, S., Pietroń, J., Bring, A., Thorslund, J. & Jarsjö, J. Present to future sediment transport of the Brahmaputra River: reducing uncertainty in predictions and management. *Reg. Environ. Chang.* **17**, 515–526 (2017).
12. Passalacqua, P., Giosan, L., Goodbred, S. & Overeem, I. Stable ≠ Sustainable: Delta

dynamics versus the human need for stability. *Earth's Futur.* **9**, e2021EF002121 (2021).
13. Kulp, S. A. & Strauss, B. H. New elevation data triple estimates of global vulnerability to sea-level rise and coastal flooding. *Nat. Commun.* **10**, (2019).
14. Cox, J. R. *et al.* A global synthesis of the effectiveness of sedimentation-enhancing strategies for river deltas and estuaries. *Glob. Planet. Change* 103796 (2022). doi:10.1016/J.GLOPLACHA.2022.103796
15. Nienhuis, J. H., Hoitink, A. J. F. T. & Törnqvist, T. E. Future Change to Tide-Influenced Deltas. *Geophys. Res. Lett.* **45**, 3499–3507 (2018).
16. Leuven, J. R. F. W., Pierik, H. J., van der Vegt, M., Bouma, T. J. & Kleinhans, M. G. Sea-level-rise-induced threats depend on the size of tide-influenced estuaries worldwide. *Nat. Clim. Chang.* **9**, 986–992 (2019).
17. Gain, A. K. *et al.* Overcoming challenges for implementing nature-based solutions in deltaic environments: Insights from the Ganges-Brahmaputra delta in Bangladesh. *Environ. Res. Lett.* **17**, (2022).
18. Mallick, B., Rogers, K. G. & Sultana, Z. In harm's way: Non-migration decisions of people at risk of slow-onset coastal hazards in Bangladesh. *Ambio* **51**, 114–134 (2022).
19. Khatun, F. *et al.* Environmental non-migration as adaptation in hazard-prone areas: Evidence from coastal Bangladesh. *Glob. Environ. Chang.* **77**, 102610 (2022).
20. Islam, M. R., Islam, M. T., Alam, M. S., Hussain, M. & Haque, M. M. Is Bhasan Char Island, Noakhali district in Bangladesh a sustainable place for the relocated Rohingya displaced people? An empirical study. *SN Soc. Sci.* **1**, 1–24 (2021).
21. Islam, M. D. & Siddika, A. Implications of the Rohingya Relocation from Cox's Bazar to Bhasan Char, Bangladesh. *Int. Migr. Rev.* (2021). doi:10.1177/01979183211064829
22. Romans, B. W., Castelltort, S., Covault, J. A., Fildani, A. & Walsh, J. P. Environmental signal propagation in sedimentary systems across timescales. *Earth-Science Rev.* **153**, 7–29 (2016).
23. D'Haen, K., Verstraeten, G. & Degryse, P. Fingerprinting historical fluvial sediment fluxes. *Prog. Phys. Geogr.* **36**, 154–186 (2012).
24. Goodbred Jr., S. L. & Kuehl, S. A. Holocene and modern sediment budgets for the Ganges-Brahmaputra river system: Evidence for highstand dispersal to flood-plain, shelf, and deep-sea depocenters. *Geology* **27**, 559–562 (1999).
25. Goodbred Jr., S. L. & Kuehl, S. A. Enormous Ganges-Brahmaputra sediment discharge during strengthened early Holocene monsoon. *Geology* **28**, 1083–1086 (2000).
26. Wang, H. *et al.* Stepwise decreases of the Huanghe (Yellow River) sediment load (1950-2005): Impacts of climate change and human activities. *Glob. Planet. Change* **57**, 331–354 (2007).
27. Miao, C., Ni, J., Borthwick, A. G. L. & Yang, L. A preliminary estimate of human and natural contributions to the changes in water discharge and sediment load in the Yellow River. *Glob. Planet. Change* **76**, 196–205 (2011).
28. Milliman, J. D. & Syvitski, J. P. M. Geomorphic / Tectonic Control of Sediment Discharge to the Ocean : The Importance of Small Mountainous Rivers. *J. Geol.* **100**, 525–544 (1992).
29. Milliman, J. D. & Meade, R. H. World-wide Delivery of River Sediment to the Oceans. *J. Geol.* **91**, 1–21 (1983).
30. Rahman, M. *et al.* Recent sediment flux to the Ganges-Brahmaputra-Meghna delta

system. *Sci. Total Environ.* **643**, 1054–1064 (2018).
31. Garzanti, E. *et al.* Mineralogical and chemical variability of fluvial sediments 1. Bedload sand (Ganga-Brahmaputra, Bangladesh). *Earth Planet. Sci. Lett.* **299**, 368–381 (2010).
32. Hay, W. W. Detrital sediment fluxes from continents to oceans. *Chem. Geol.* **145**, 287–323 (1998).
33. Syvitski, J. P. M. & Saito, Y. Morphodynamics of deltas under the influence of humans. *Glob. Planet. Change* **57**, 261–282 (2007).
34. Sinha, R., Singh, S., Mishra, K. & Swarnkar, S. Channel morphodynamics and sediment budget of the Lower Ganga River using a hydro-geomorphological approach. *Earth Surf. Process. Landforms* 1–20 (2022). doi:10.1002/esp.5325
35. Szabo, S. *et al.* Population dynamics, delta vulnerability and environmental change: comparison of the Mekong, Ganges–Brahmaputra and Amazon delta regions. *Sustain. Sci.* **11**, 539–554 (2016).
36. Anderson, D. M., Overpeck, J. T. & Gupta, A. K. Increase in the Asian Southwest Monsoon During the Past Four Centuries. *Science (80-.).* **297**, 596–599 (2002).
37. Caesar, J., Janes, T., Lindsay, A. & Bhaskaran, B. Temperature and precipitation projections over Bangladesh and the upstream Ganges, Brahmaputra and Meghna systems. *Environ. Sci. Process. Impacts* **17**, 1047–1056 (2015).
38. Mishra, V. & Lilhare, R. Hydrologic sensitivity of Indian sub-continental river basins to climate change. *Glob. Planet. Change* **139**, 78–96 (2016).
39. Sandeep, K. *et al.* A multi-proxy lake sediment record of Indian summer monsoon variability during the Holocene in southern India. *Palaeogeogr. Palaeoclimatol. Palaeoecol.* **476**, 1–14 (2017).
40. Sarkar, S. *et al.* Monsoon source shifts during the drying mid-Holocene: Biomarker isotope based evidence from the core 'monsoon zone' (CMZ) of India. *Quat. Sci. Rev.* **123**, 144–157 (2015).
41. Kudrass, H. R., Hofmann, A., Doose, H., Emeis, K. & Erlenkeuser, H. Modulation and amplification of climatic changes in the Northern Hemisphere by the Indian summer monsoon during the past 80 k.y. *Geology* **29**, 63–66 (2001).
42. Banerji, U. S., Arulbalaji, P. & Padmalal, D. Holocene climate variability and Indian Summer Monsoon: An overview. *Holocene* **30**, 744–773 (2020).
43. Wang, Y. *et al.* Abrupt mid-Holocene decline in the Indian Summer Monsoon caused by tropical Indian Ocean cooling. *Clim. Dyn.* **55**, 1961–1977 (2020).
44. Misra, P., Tandon, S. K. & Sinha, R. Holocene climate records from lake sediments in India: Assessment of coherence across climate zones. *Earth-Science Rev.* **190**, 370–397 (2019).
45. Zhao, C. *et al.* Paleoclimate Significance of Reconstructed Rainfall Isotope Changes in Asian Monsoon Region. *Geophys. Res. Lett.* **48**, 1–13 (2021).
46. IPCC. *Climate Change 2014: Synthesis Report. Contribution of Working Groups I, II and III to the Fifth Assessment Report of the Intergovernmental Panel on Climate Change [Core Writing Team, R.K. Pachauri and L.A. Meyer (eds.)].* (IPCC, 2014).
47. IPCC. *Climate Change 2022: Impacts, Adaptation, and Vulnerability. Contribution of Working Group II to the Sixth Assessment Report of the Intergovernmental Panel on Climate Change [H.-O. Pörtner, D.C. Roberts, M. Tignor, E.S. Poloczanska, K. Mintenbeck, A. Aleg*. (Cambridge University Press, 2022).

48. Lutz, A. F., Immerzeel, W. W., Shrestha, A. B. & Bierkens, M. F. P. Consistent increase in High Asia's runoff due to increasing glacier melt and precipitation. *Nat. Clim. Chang.* **4**, 587–592 (2014).
49. Akter, J., Sarker, M. H., Popescu, I. & Roelvink, D. Evolution of the Bengal Delta and Its Prevailing Processes. *J. Coast. Res.* **321**, 1212–1226 (2016).
50. Sinha, R., Singh, S., Mishra, K. & Swarnkar, S. Channel morphodynamics and sediment budget of the Lower Ganga River using a hydro-geomorphological approach. *Earth Surf. Process. Landforms* 0–2 (2022). doi:10.1002/esp.5325
51. Oppenheimer, M. *et al.* Sea Level Rise and Implications for Low-Lying Islands, Coasts and Communities. in *IPCC Special Report on the Ocean and Cryosphere in a Changing Climate* (eds. Pörtner, H.-O. et al.) 321–445 (Cambridge University Press, 2019). doi:https://doi.org/10.1017/9781009157964.006.
52. Weber, M. E., Wiedicke, M. H., Kudrass, H. R., Hübscher, C. & Erlenkeuser, H. Active growth of the Bengal Fan during sea-level rise and highstand. *Geology* **25**, 315–318 (1997).
53. Kottke, B. *et al.* Acoustic facies and depositional processes in the upper submarine canyon Swatch of No Ground (Bay of Bengal). *Deep. Res. Part II Top. Stud. Oceanogr.* **50**, 979–1001 (2003).
54. Fournier, L. *et al.* The Bengal fan: External controls on the Holocene Active Channel turbidite activity. *The Holocene* **7**, 900–913 (2017).
55. Bendixen, M., Best, J., Hackney, C. & Iversen, L. L. Time is running out for sand. *Nature* **571**, 29–31 (2019).
56. Hackney, C. R. *et al.* River bank instability from unsustainable sand mining in the lower Mekong River. *Nat. Sustain.* **3**, 217–225 (2020).
57. Goodbred Jr., S. L. *et al.* Piecing together the Ganges-Brahmaputra-Meghna river delta: Use of sediment provenance to reconstruct the history and interaction of multiple fluvial systems during Holocene delta evolution. *Bull. Geol. Soc. Am.* **126**, 1495–1510 (2014).
58. Singh, S. K., Rai, S. K. & Krishnaswami, S. Sr and Nd isotopes in River sediments from the Ganga basin: Sediment provenance and spatial variability in physical erosion. *J. Geophys. Res. Earth Surf.* **113**, 1–18 (2008).
59. Singh, S. K. & France-Lanord, C. Tracing the distribution of erosion in the Brahmaputra watershed from isotopic compositions of stream sediments. *Earth Planet. Sci. Lett.* **202**, 645–662 (2002).
60. Islam, M. R., Begum, S. F., Yamaguchi, Y. & Ogawa, K. The Ganges and Brahmaputra rivers in Bangladesh: basin denudation and sedimentation. *Hydrol. Process.* **13**, 2907–2923 (1999).
61. Lupker, M. *et al.* A Rouse-based method to integrate the chemical composition of river sediments: Application to the Ganga basin. *J. Geophys. Res. Earth Surf.* **116**, 1–24 (2011).
62. Cecil, C. B., Edgar, N. T., Dulong, F. T. & Neuzil, S. G. Concepts, Models, and Examples of Climatic Controls on Sedimentation: Introduction. in *Climate Controls on Stratigraphy* 5–8 (SEPM (Society for Sedimentary Geology), 2003). doi:https://doi.org/10.2110/pec.03.77.0005
63. Kääb, A., Berthier, E., Nuth, C., Gardelle, J. & Arnaud, Y. Contrasting patterns of early twenty-first-century glacier mass change in the Himalayas. *Nature* **488**, 495–498 (2012).
64. Gibling, M. R., Tandon, S. K., Sinha, R. & Jain, M. Discontinuity-bounded alluvial sequences

of the southern Gangetic plains, India: Aggradation and degradation in response to monsoonal strength. *J. Sediment. Res.* **75**, 369–385 (2005).
65. Goodbred, S. L. Response of the Ganges dispersal system to climate change: a source-to-sink view since the last interstade. *Sediment. Geol.* **162**, 83–104 (2003).
66. Williams, M. A. J. & Clarke, M. F. Late Quaternary environments in north-central India. *Nature* **308**, 633–635 (1984).
67. Simpson, G. & Castelltort, S. Model shows that rivers transmit high-frequency climate cycles to the sedimentary record. *Geology* **40**, 1131–1134 (2012).
68. Clift, P. D. *et al.* Holocene erosion of the Lesser Himalaya triggered by intensified summer monsoon. *Geology* **36**, 79–82 (2008).
69. Sarkar, M. H. & Thorne, C. R. Morphological Response of the Brahmaputra–Padma–Lower Meghna River System to the Assam Earthquake of 1950. in *Braided Rivers* (eds. Jarvis, I., Sambrook Smith, G. H., Best, J. L., Bristow, C. S. & Petts, G. E.) 289–310 (Blackwell Publishing Ltd., 2009). doi:https://doi.org/10.1002/9781444304374.ch14
70. Lahiri, S. K. & Sinha, R. Tectonic controls on the morphodynamics of the Brahmaputra River system in the upper Assam valley, India. *Geomorphology* **169**–**170**, 74–85 (2012).
71. Allison, M. A. Historical changes in the Ganges-Brahmaputra delta front. *J. Coast. Res.* **14**, 1269–1275 (1998).
72. Brammer, H. Bangladesh's dynamic coastal regions and sea-level rise. *Clim. Risk Manag.* **1**, 51–62 (2014).
73. Sarwar, M. G. M. & Woodroffe, C. D. Rates of shoreline change along the coast of Bangladesh. *J. Coast. Conserv.* **17**, 515–526 (2013).
74. Dunn, F. E. & Minderhoud, P. S. J. Sedimentation strategies provide effective but limited mitigation of relative sea-level rise in the Mekong delta. *Commun. Earth Environ.* **3**, (2022).
75. Smajgl, A. *et al.* Responding to rising sea levels in the Mekong Delta. *Nat. Clim. Chang.* **5**, 167–174 (2015).
76. Rogers, K. G. & Overeem, I. Doomed to drown? Sediment dynamics in the human-controlled floodplains of the active Bengal Delta. *Elementa* **5**, (2017).
77. Paprocki, K. All That Is Solid Melts into the Bay: Anticipatory Ruination and Climate Change Adaptation. *Antipode* **51**, 295–315 (2019).
78. Auerbach, L. W. *et al.* Flood risk of natural and embanked landscapes on the Ganges–Brahmaputra tidal delta plain. *Nat. Clim. Chang.* **5**, 153–157 (2015).
79. Pethick, J. & Orford, J. D. Rapid rise in effective sea-level in southwest Bangladesh: Its causes and contemporary rates. *Glob. Planet. Change* **111**, 237–245 (2013).
80. Rahman, M. M. *et al.* Sustainability of the coastal zone of the Ganges-Brahmaputra-Meghna delta under climatic and anthropogenic stresses. *Sci. Total Environ.* **829**, 154547 (2022).
81. Barbour, E. J. *et al.* The unequal distribution of water risks and adaptation benefits in coastal Bangladesh. *Nat. Sustain.* **5**, 294–302 (2022).
82. Bomer, E. J., Wilson, C. A., Hale, R. P., Hossain, A. N. M. & Rahman, F. M. A. Surface elevation and sedimentation dynamics in the Ganges-Brahmaputra tidal delta plain, Bangladesh: Evidence for mangrove adaptation to human-induced tidal amplification. *Catena* **187**, 104312 (2020).

83. Akter, J., Roelvink, D. & van der Wegen, M. Process-based modeling deriving a long-term sediment budget for the Ganges-Brahmaputra-Meghna Delta, Bangladesh. *Estuar. Coast. Shelf Sci.* **260**, 107509 (2021).
84. Paszkowski, A., Goodbred, S., Borgomeo, E., Khan, M. S. A. & Hall, J. W. Geomorphic change in the Ganges–Brahmaputra–Meghna delta. *Nat. Rev. Earth Environ. 2021* 1–18 (2021). doi:10.1038/s43017-021-00213-4
85. Rampini, C. Hydropower and Sino-Indian Hydropolitics Along the Yarlung-Tsangpo-Brahmaputra. in *The Political Economy of Hydropower in Southwest China and Beyond* (eds. Rousseau, J. & Habich-Sobiegalla, S.) 235–254 (Palgrave Macmillan, Cham, 2021). doi:10.1007/978-3-030-59361-2_12
86. Grumbine, R. E. & Pandit, M. K. Threats from India's Himalaya dams. *Science (80-.).* **339**, 36–37 (2013).
87. Menon, M. & Kohli, K. From impact assessment to clearance manufacture. *Econ. Polit. Wkly.* **44**, 20–23 (2009).
88. Singh, J. S. Sustainable development of the Indian Himalayan region: Linking ecological and economic concerns. *Curr. Sci.* **90**, 784–788 (2006).
89. Agrawal, R. Polluters Rewarded. *countercurrents.org* (2008). Available at: https://countercurrents.org/agrawal040308.htm.
90. Arora, N. & Ghoshal, D. India plans dam on Brahmaputra to offset Chinese construction upstream. *Reuters* (2020). Available at: https://www.reuters.com/article/us-india-china-hydropower-idUKKBN28B4NN.
91. Li, D. *et al.* Exceptional increases in fluvial sediment fluxes in a warmer and wetter High Mountain Asia. *Science (80-.).* **374**, 599–603 (2021).
92. Dewan, C. *Misreading the Bengal Delta - Climate Change, Development, and Livelihoods in Coastal Bangladesh*. (University of Washington Press, 2022).
93. Gain, A. K. *et al.* Overcoming challenges for implementing nature-based solutions in deltaic environments: insights from the Ganges-Brahmaputra delta in Bangladesh. *Environ. Res. Lett.* **17**, 64052 (2022).
94. Grimaud, J. L. *et al.* Flexural deformation controls on Late Quaternary sediment dispersal in the Garo-Rajmahal Gap, NW Bengal Basin. *Basin Res.* **32**, 1252–1270 (2020).
95. Pickering, J. L. *et al.* Terrace formation in the upper Bengal basin since the Middle Pleistocene: Brahmaputra fan delta construction during multiple highstands. *Basin Res.* **30**, 550–567 (2018).
96. Pickering, J. L. *et al.* Late Quaternary sedimentary record and Holocene channel avulsions of the Jamuna and Old Brahmaputra River valleys in the upper Bengal delta plain. *Geomorphology* **227**, 123–136 (2014).
97. Sincavage, R., Goodbred, S. & Pickering, J. Holocene Brahmaputra River path selection and variable sediment bypass as indicators of fluctuating hydrologic and climate conditions in Sylhet Basin , Bangladesh. 302–320 (2018). doi:10.1111/bre.12254
98. Ayers, J. C. *et al.* Sources of salinity and arsenic in groundwater in southwest Bangladesh. *Geochem. Trans.* **17**, 1–22 (2016).
99. Ahmed, M. K., Islam, S., Rahman, M. S., Haque, M. R. & Islam, M. M. Heavy Metals in Water , Sediment and Some Fishes of Buriganga River, Bangladesh. *Int. J. Environ. Res.* **4**, 321–332 (2010).

100. BADC (Bangladesh Agricultural Development Corporation). Deep Tubewell II Project: Final Reports. (1992).
101. Khan, S. R. & Islam, B. Holocene stratigraphy of the lower Ganges-Brahmaputra river delta in Bangladesh. *Front. Earth Sci. China* **2**, 393–399 (2008).
102. Michels, K. H., Kudrass, H. R., Hübscher, C., Suckow, A. & Wiedicke, M. The submarine delta of the Ganges-Brahmaputra: Cyclone-dominated sedimentation patterns. *Mar. Geol.* **149**, 133–154 (1998).
103. Palamenghi, L., Schwenk, T., Spiess, V. & Kudrass, H. R. Seismostratigraphic analysis with centennial to decadal time resolution of the sediment sink in the Ganges-Brahmaputra subaqueous delta. *Cont. Shelf Res.* **31**, 712–730 (2011).
104. Sarkar, A. *et al.* Evolution of Ganges-Brahmaputra western delta plain: Clues from sedimentology and carbon isotopes. *Quat. Sci. Rev.* **28**, 2564–2581 (2009).
105. Pickering, J. L. *et al.* Impact of glacial-lake paleofloods on valley development since glacial termination II : A conundrum of hydrology and scale for the lowstand Brahmaputra-Jamuna paleovalley system a Mt. (2018).
106. Shamsudduha, M., Uddin, A., Saunders, J. A. & Lee, M. K. Quaternary stratigraphy, sediment characteristics and geochemistry of arsenic-contaminated alluvial aquifers in the Ganges-Brahmaputra floodplain in central Bangladesh. *J. Contam. Hydrol.* **99**, 112–136 (2008).
107. Pate, R. D., Goodbred, S. L. & Khan, S. R. Delta Double-Stack: Juxtaposed Holocene and Pleistocene Sequences from the Bengal Basin, Bangladesh. *Sediment. Rec.* **7**, 4–9 (2009).
108. DPHE-JICA (Department of Public Health Engineering and Japanese International Cooperation Agency). *Development of deep aquifer database and preliminary deep aquifer map. Final Report.* (2006).
109. (JICA), J. I. C. A. Geology and Stone material, Part 1: Geology. in **6**, 133 (Japan International Cooperation Agency, 1976).
110. Ghosal, U., Sikdar, P. K. & McArthur, J. M. Palaeosol Control of Arsenic Pollution: The Bengal Basin in West Bengal, India. *Groundwater* **53**, 588–599 (2015).
111. Hait, A. K. *et al.* New dates of Pleisto-Holocene subcrop samples from South Bengal, India. *Indian J. Earth Sci.* **23**, 79–82 (1996).
112. Hoque, M. A., McArthur, J. M. & Sikdar, P. K. The palaeosol model of arsenic pollution of groundwater tested along a 32km traverse across West Bengal, India. *Sci. Total Environ.* **431**, 157–165 (2012).
113. Hoque, M. A., Mcarthur, J. M. & Sikdar, P. K. Sources of low-arsenic groundwater in the Bengal Basin: investigating the influence of the last glacial maximum palaeosol using a 115-km traverse across Bangladesh. *Hydrogeol. J.* **22**, 1535–1547 (2014).
114. Goodbred, Jr., S. L. *et al.* Piecing together the Ganges-Brahmaputra-Meghna River delta: Use of sediment provenance to reconstruct the history and interaction of multiple fluvial systems during Holocene delta evolution. *Geol. Soc. Am. Bull.* **126**, 1495–1510 (2014).
115. Grall, C. *et al.* A base-level stratigraphic approach to determining Holocene subsidence of the Ganges–Meghna–Brahmaputra Delta plain. *Earth Planet. Sci. Lett.* **499**, 23–36 (2018).
116. Sincavage, R., Goodbred, S. & Pickering, J. Holocene Brahmaputra River path selection and variable sediment bypass as indicators of fluctuating hydrologic and climate conditions in Sylhet Basin, Bangladesh. *Basin Res.* **30**, 302–320 (2018).

117. Sincavage, R. S., Paola, C. & Goodbred, S. L. Coupling Mass Extraction and Downstream Fining With Fluvial Facies Changes Across the Sylhet Basin of the Ganges-Brahmaputra-Meghna Delta. *J. Geophys. Res. Earth Surf.* **124**, 400–413 (2019).
118. Reitz, M. D. *et al.* Effects of tectonic deformation and sea level on river path selection: Theory and application to the Ganges-Brahmaputra-Meghna River Delta. *J. Geophys. Res. Earth Surf.* **120**, 671–689 (2015).
119. Goodbred, S. L. *et al.* Piecing together the Ganges-Brahmaputra-Meghna river delta: Use of sediment provenance to reconstruct the history and interaction of multiple fluvial systems during Holocene delta evolution. *Bull. Geol. Soc. Am.* **126**, 1495–1510 (2014).
120. Lambeck, K., Rouby, H., Purcell, A., Sun, Y. & Sambridge, M. Sea level and global ice volumes from the Last Glacial Maximum to the Holocene. *Proc. Natl. Acad. Sci. U. S. A.* **111**, 15296–15303 (2014).
121. Kuehl, S. A., Levy, B. M., Moore, W. S. & Allison, M. A. Subaqueous delta of the Ganges-Brahmaputra river system. *Mar. Geol.* **144**, 81–96 (1997).
122. Garzanti, E. *et al.* Provenance of Bengal Shelf Sediments: 2. Petrology and Geochemistry of Sand. *Minerals* **9**, 642 (2019).
123. Lupker, M., France-Lanord, C., Galy, V., Lavé, J. & Kudrass, H. Increasing chemical weathering in the Himalayan system since the Last Glacial Maximum. *Earth Planet. Sci. Lett.* **365**, 243–252 (2013).
124. Stanley, D. J. & Hait, A. K. Holocene depositional patterns, neotectonics and Sundarban mangroves in the western Ganges-Brahmaputra delta. *J. Coast. Res.* **16**, 26–39 (2000).
125. Wilson, C. A. & Goodbred Jr., S. L. Construction and Maintenance of the Ganges-Brahmaputra-Meghna Delta: Linking Process, Morphology, and Stratigraphy. *Ann. Rev. Mar. Sci.* **7**, 67–88 (2015).
126. Rogers, K. G., Goodbred, S. L. & Mondal, D. R. Monsoon sedimentation on the 'abandoned' tide-influenced Ganges-Brahmaputra delta plain. *Estuar. Coast. Shelf Sci.* **131**, 297–309 (2013).
127. Pate, R. D. Multiple-proxy records of delta evolution and dispersal system behavior: fluvial and coastal borehole evidence from the Bengal Basin, Bangladesh. (Vanderbilt University, 2008).
128. Ullah, M. S. Provenance analysis and depositional system of the Late Quaternary sediment from the Ganges-Brahmaputra (G-B) delta, Bangladesh: Application of strontium geochemistry. (Vanderbilt University, 2010).
129. Woodruff, J. D., Irish, J. L. & Camargo, S. J. Coastal flooding by tropical cyclones and sea-level rise. *Nature* **504**, 44–52 (2013).
130. Kay, S. *et al.* Modelling the increased frequency of extreme sea levels in the Ganges–Brahmaputra–Meghna delta due to sea level rise and other effects of climate change. *Environ. Sci. Process. Impacts* **17**, 1311–1322 (2015).
131. Tessler, Z. D., Vörösmarty, C. J., Overeem, I. & Syvitski, J. P. M. A model of water and sediment balance as determinants of relative sea level rise in contemporary and future deltas. *Geomorphology* **305**, 209–220 (2018).
132. Clemens, S. C. *et al.* Remote and local drivers of Pleistocene South Asian summer monsoon precipitation : A test for future predictions. *Sci. Adv.* **7**, eabg3848 (2021).

ACKNOWLEDGEMENTS

This work was supported in part by U.S. National Science Foundation grants OISE-0968354 to S.L.G., M.S.S., and C.P., RISE-1342946 to S.L.G., OCE-1600319 to S.L.G., J.C.A., J.M.G., OCE-1600258 to C.A.W., BCS-1716909 to C.A.W., K.G.R., and J.M.G., and U.S. Office of Naval Research grant N00014-11-1-0683 to S.L.G., J.C.A., M.S.S. and J.M.G. The authors also thank contributions from Rachel L. Bain and Thomas R. Hartzog and field support from the Department of Geology, University of Dhaka and Nazrul Islam Bachchu of Pugmark Tours and Travels.

AUTHOR CONTRIBUTION STATEMENT

S.L.G., C.P., and M.S.S. designed the original project, and all authors contributed to its intellectual development and success. J.L.R., J.L.P., R.S.S., M.S.H., C.A.W., D.R.M., J.-L.G., C.J.G., K.G.R., M.D., R.P.H., M.G.M., and L.A.W. conducted the field sampling and lab analyses. J.L.R., S.L.G., J.L.P., R.S.S., and C.A.W. developed and analyzed the dataset. J.L.R. and S.L.G. wrote the manuscript with contributions from J.L.P., R.S.S., J.C.A., C.A.W., C.P., M.S.S., C.J.G., K.G.R., E.A.C., and R.P.H. All authors reviewed and commented on the manuscript.

COMPETING INTERESTS STATEMENT

The authors declare no competing interests.

Figure 1. Map of Bengal basin and the Ganges-Brahmaputra River (G-B) delta in South Asia showing the study area and sampling and data locations. The G-B delta and lower Ganges and Brahmaputra rivers are located in Bangladesh and West Bengal, India. The Holocene delta developed on an incised Pleistocene surface and the boundary of Holocene deposits is shown by the black dashed line. The subaqueous portion of the Holocene delta is located on the shelf and bordered by the Swatch of No Ground canyon and Bay of Bengal to the south. Over 450 boreholes from this study are denoted by the dark and light gray--filled circles [115,127,128], with the light gray circles demarking Transect G cores shown in Figure S3. Core and acoustic-flection data from other studies used to define the thickness and extent of Holocene delta deposits are shown by white-filled circles [99–104,106,108,110–112]. The border of Bangladesh is outlined in pink, and the pink-shaded region represents the higher-risk coastal zone based on the model domain used in Akter et al. (2021) [83]. World Ocean Base layer is from Esri, GEBCO, NOAA NGDC, HERE, Garmin, and other contributors; the world countries shapefile is from Esri, Garmin International, Inc., and the U.S. Central Intelligence Agency (The World Factbook); and the hydrology shapefiles (World Water Bodies and World Linear Water) are from Esri and Garmin International, Inc.

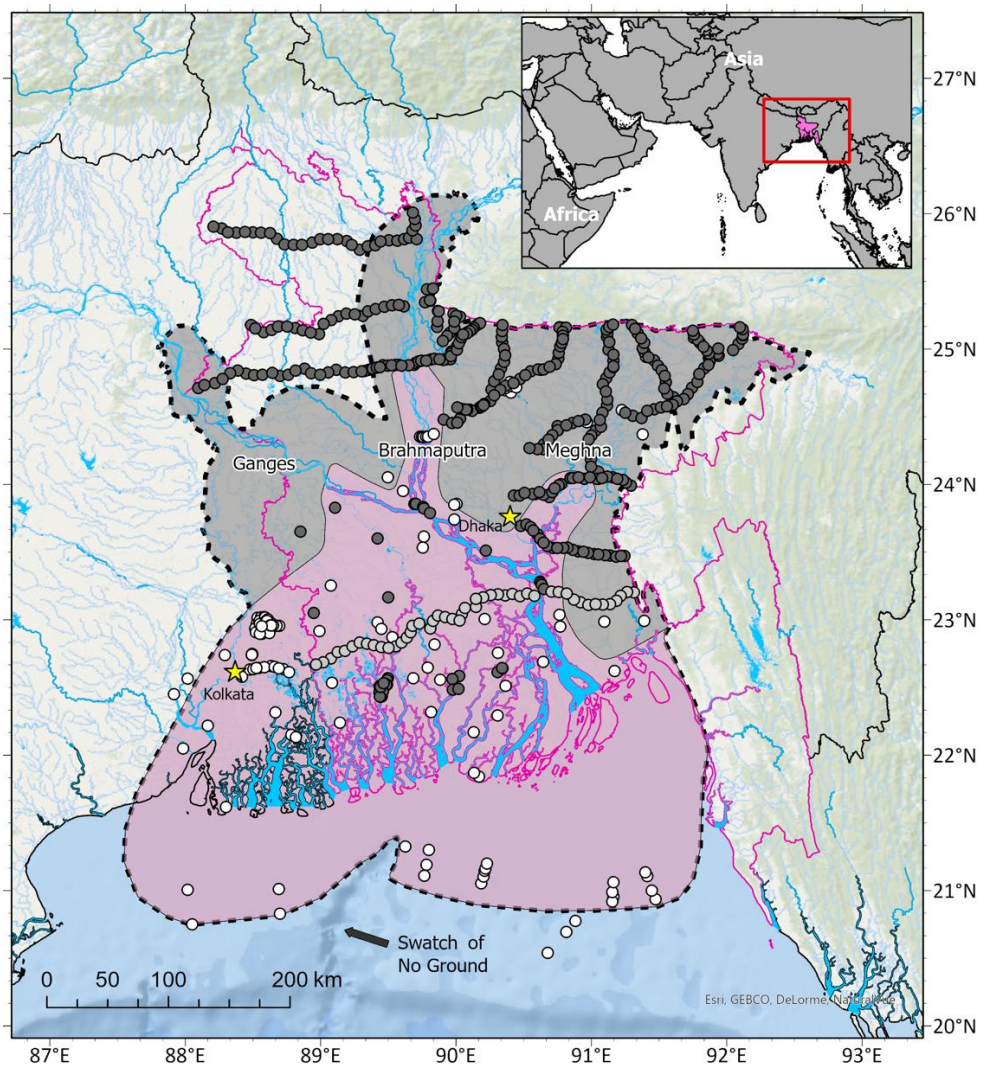

Table 1. STILL GOING TO UPDATE THIS TABLE TO REMOVE the 'a' onshore-only values and just include the 'b' total values for the 6-0 and 8-6 ka periods. Average mass storage rates and grain size distributions for deposits stored on the Ganges-Brahmaputra delta over the last 12 kyr. Highest rates of sediment delivery and storage in the delta occur between 10—8 ka and correspond with a sandier sediment load.

Years	Mud (Mt/yr) (<62.5 µm)	Fine sand (Mt/yr) (62.5-250 µm)	Medium-coarse sand (Mt/yr) (250-1000 µm)
6-0 ka [a]	226	249	137
6-0 ka [b]	389	294	162
8-6 ka [a]	262	474	284
8-6 ka [b]	425	519	309
10-8 ka	505	824	671
12-10 ka	171	277	371

[a] Onshore material only included. [b] Offshore mass distributed with 75% of material contained in the 6-0 ka unit and 25% of material contained in the 8-6 ka unit.

Table 2. Average mass storage rates and percent contribution for each river system throughout the Holocene. The Brahmaputra is the main contributor of sediment in the early-mid Holocene (12–6 ka), while the Ganges delivers most of the sediment over the last 6 kyr. Storage rate data are plotted in Figure 2C.

6–0 ka		
Source	**Storage Rate (Mt/yr)**	**Percent Contribution**
Ganges	426	50.4%
Brahmaputra	377	44.7%
Mixed G+B	7	0.8%
Other	35	4.1%
Total	845	

8–6 ka		
Source	**Storage Rate (Mt/yr)**	**Percent Contribution**
Ganges	308	24.6%
Brahmaputra	726	58.0%
Mixed G+B	17	1.3%
Other	202	16.1%
Total	1253	

10–8 ka		
Source	**Storage Rate (Mt/yr)**	**Percent Contribution**
Ganges	413	20.7%
Brahmaputra	1119	55.9%
Mixed G+B	128	6.4%
Other	340	17.0%
Total	2001	

12–10 ka		
Source	**Storage Rate (Mt/yr)**	**Percent Contribution**
Ganges	116	14.2%
Brahmaputra	512	62.6%
Mixed G+B	16	2.0%
Other	174	21.2%
Total	818	

Figure 2. Changes in paleosalinity (A) and atmospheric moisture (B) correspond with observed changes in the mass and caliber (C-D) of sediment stored on the Ganges-Brahmaputra delta. A) A paleosalinity record from sediment cores collected in the northern Bay of Bengal [41] provides a proxy record for an enhanced early Holocene monsoon, when runoff and river discharge increased and lowered salinity of the surface mixed layer. Salinities decrease after 6 ka under weakening monsoon precipitation and reduced (but still large) river discharge. B) Terrestrial records of leaf-wax stable carbon isotopes from lacustrine sediments in Lonar Lake, central India [40] provide evidence for increased atmospheric moisture during the early Holocene Climatic Optimum (~9-5 ka), with sharply decreasing moisture levels with monsoon weakening after ~6 ka. C) In the early Holocene, most sediment was deposited by the Brahmaputra river, followed by the Ganges. For the last 6 kyr, the two rivers have deposited a roughly equivalent mass of sediment on the delta but with few deposits reflecting any mixing between them. Other tributary sources have locally contributed sediment to the delta, but the amount is comparatively minor. Observed sediment delivery rates over the Holocene are denoted in white boxes and the reconstruction of the maximum potential reconstructed sediment load based on bypassing estimates are shown in gray text within the dashed boxes.

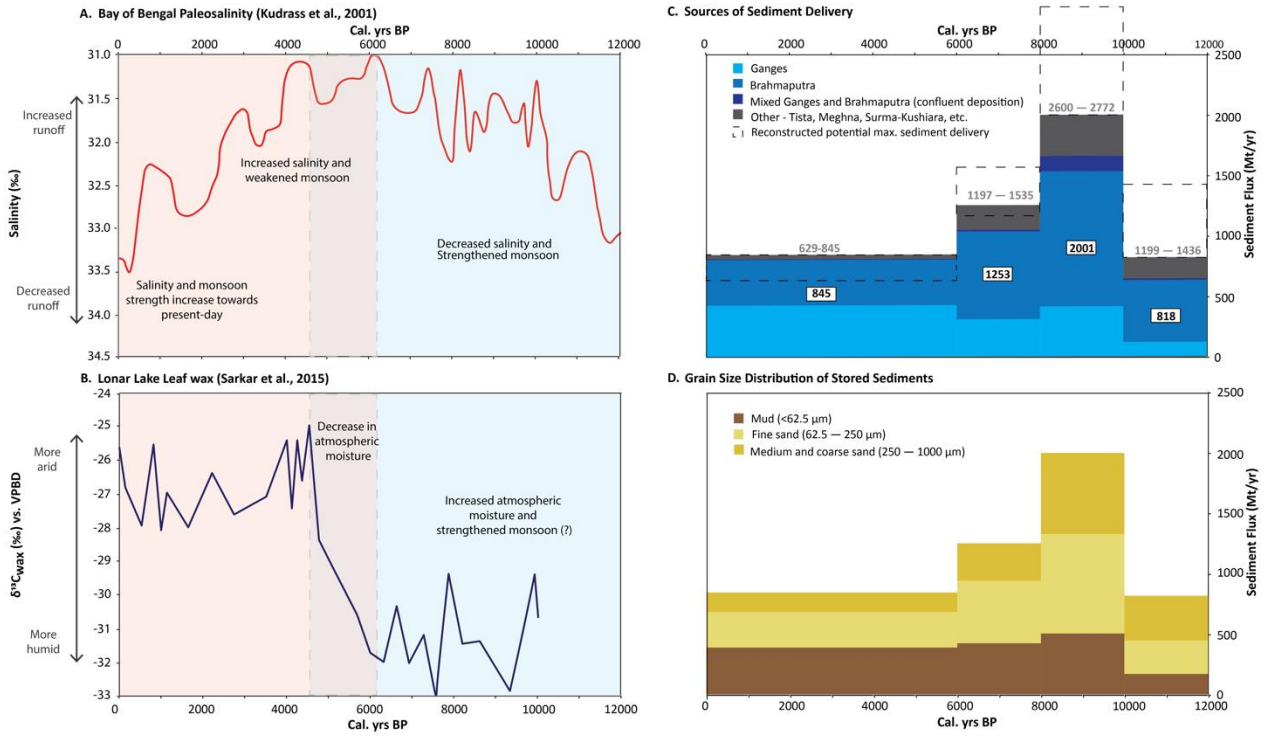

Figure 3. Modern, Holocene, and future mass-balance calculations comparing rates of sediment delivery against the mass required to offset sea-level rise and subsidence. (A) Summary of the mass-balance scenarios, showing input values for sediment supply and sea-level rise and the calculated outputs for *Δ Mass* and $f_{(supply)}$. Calculations of required mass for each scenario can be found in Table S4. (B) An explanation of the calculated terms, the conditions for each *Δ Mass* case, and the data sources are provided along with (C) a schematic diagram of the mass-balance model for the delta. The Holocene: 10-8 ka scenario considers only the high sediment demand case, as the whole delta aggraded in response to rapid sea-level rise during this period.

A

Scenario	Supply (Mt/yr)	S.L. Rise (mm/yr)	*Δ Mass* (Mt/yr) low	*Δ Mass* (Mt/yr) medium	*Δ Mass* (Mt/yr) high	$f_{(supply)}$ medium
20th century: typical Q_s	1,100 [a]	2.5 [f]	367	232	88	27%
20th century: low Q_s	700 [a]	2.5 [f]	-33	-168	-313	-19%
Holocene: 6-0 ka	845 [b]	0.5 [g]	419	344	283	69%
Holocene: 8-6 ka	1,253 [b]	4.8 [g]	384	220	29	21%
Holocene: 10-8 ka	2,001 [b]	12.5 [g]	--	--	792	66% (high)
2050 climate only [a]	1,349 [c]	5.6 [f]	139	-89	-361	-6%
2100 climate only [a]	1,624 [c]	8.5 [f]	-32	-347	-739	-18%
River-linking (partial) [b]	866 [d]	8.5 [f]	-790	-1,105	-1,497	-56%
River-linking (all) [b]	600 [d]	8.5 [f]	-1,056	-1,371	-1,763	-70%
2100 full impacts [c]	85 [e]	8.5 [f]	-1,571	-1,886	-2,278	-96%

C

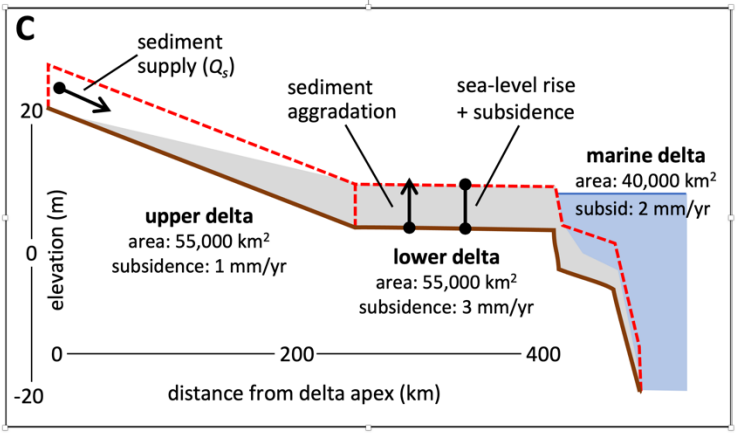

B

CALCULATED TERMS:

Δ Mass = $Mass_{(supply)}$ - $Mass_{(required)}$ where:

- $Mass_{(required)}$ = $SUM[Area_{(sub\text{-}region)} \times RSLR_{(sub\text{-}region)}]$ for each sub-region *upper, lower, and marine*
- $RSLR_{(sub\text{-}reg)}$ = *Eustatic SLR + Subsidence*$_{(sub\text{-}reg)}$

$f_{(supply)}$ = fraction of sediment supply for which delta is in excess or deficit (medium sediment case only)

Δ-MASS CASES:

- **low sediment demand** = the lower delta aggrades at the pace of RSLR, with the upper and marine deltas aggrading at 0.5 x RSLR – allows some non-deposition in higher portions of upper delta and some likely coastal erosion and ravinement of shelf.
- **medium sediment demand** = the lower delta and marine area receive full aggradation to offset RLSR and protect the coast, and the upper delta accretes at 0.5 x RSLR – a reasonable scenario to maintain shoreline stability and limit lower-delta flooding.
- **high sediment demand** = the entire delta requires full aggradation to offset RSLR – less likely scenario requiring all areas to receive maximum sediment.

SUPPLY and SEA-LEVEL RISE SCENARIOS:

[a] Rahman et al. (2018), *Sci. Tot. Enviro.*, **643**:1054.
[b] this study
[c] Darby et al. (2015), *Enviro. Science*, **17**:1587.
[d] Higgins et al. (2018), *Elementa*, **6**:20.
[e] Dunn et al. (2019), *Enviro. Res. Letters*, **14**:084034.
[f] IPCC (2019), *Cambridge Press*, SROCC Chapter 4.
[g] Lambeck et al. (2014), *PNAS*, **111**(43):15296.

Figure 4. A) Comparison of future changes in sea level (shown relative to 1992 CE) [129] to B) Holocene changes in global sea level (shown relative to EGM96) [120]. Local sea level (not shown) [130] and relative sea level is expected to rise by ~1 m by 2100 (blue line, panel A). C) In the future, predicted changes in monsoon strength [1] and river damming with the National River Linking Project (NRLP) [3,131] indicate that sediment fluxes reaching the delta may increase or be reduced. Minimum required sediment delivery is calculated using the whole delta area (Table S4), so less sediment delivery may still sustain the at-risk portions of the delta against rising sea level. D) The rate of sediment storage on the delta exceeded the necessary sediment required to keep pace with sea level between 10–8 ka, and for the last 8 ka, whole-delta storage rates have closely matched or exceeded sediment requirements contributing to progradation of the delta. Ultimately, changes in sediment delivery to the delta are likely to occur from river damming [3,131], sand mining (Sickmann et al., in prep), strengthening monsoon [132], and anthropogenic climate change [1,132].